CERN 97–07
3 July 1997

ORGANISATION EUROPÉENNE POUR LA RECHERCHE NUCLÉAIRE
CERN EUROPEAN ORGANIZATION FOR NUCLEAR RESEARCH

CALIBRATION OF SECONDARY EMISSION MONITORS OF ABSOLUTE PROTON BEAM INTENSITY IN THE CERN SPS NORTH AREA

K. Bernier, G. de Rijk, G. Ferioli, E. Hatziangeli, A. Marchionni, V. Palladino,
G.R. Stevenson, T. Tabarelli de Fatis, E. Tsesmelis

GENEVA
1997

CERN–Service d'information scientifique–RD/976–2000–octobre–1997

ISSN 0007–8328
ISBN 92–9083–118–9

ABSTRACT

Secondary Emission Monitors (SEMs) are used at the SPS for measurements of the absolute proton beam intensity. As an accurate measurement was recently required by the NA56 (SPY) experiment, the responses of all the SEMs used in the SPS North Area, including those used for NA56, were calibrated. The independent measurement of the absolute proton intensity needed for this calibration was obtained by an activation method, where the radioactivity induced in a thin aluminium foil is measured with a gamma counter immediately after a short exposure of the foil to the proton beam. The foil activity was in turn calibrated using the absolute proton intensity measurements provided by the Beam Current Transformers (BCTs) available in the West Area Neutrino Facility. A description of the experimental method and results of the calibration are given. SEM calibration factors were determined with an error that, even in the worst case, does not exceed 3%. The response per unit proton intensity of the new titanium SEMs installed in 1995 is about 9% smaller than that of the traditional aluminium SEMs. The measured calibration factor of the titanium monitor used by NA56 has been shown to be stable within ±1% over a period of almost one month. By combining this additional uncertainty to the error on the determination of the calibration factor from the activation measurement, the absolute proton intensity delivered to NA56 could be measured with an uncertainty of 1.7%.

CONTENTS

1 INTRODUCTION

In the spring of 1996, experiment NA56 (SPY) [1] was performed in the H6 beam in the CERN SPS North Area, with the aim of measuring absolute production rates of π's and K's from collisions of 450 Gev/c protons on various beryllium targets. Protons extracted from the SPS in the TT20 transfer tunnel towards the North Area with a slow resonant extraction of 2.6 s duration are distributed by two splitter stations over three branches serving the targets T2, T4, and T6 [Fig. 1(a)] in the target hall TCC2. The H6 is an unseparated secondary beam produced from targets housed in the T4 target station. Slow extraction is required to limit the instantaneous trigger rate and it is anyway the only extraction scheme currently available in the SPS North Area.

The SPY experiment required a few per cent absolute measurement of the proton intensity incident on T4. A very accurate determination (of the order of 1%) of absolute proton intensity is achievable in fast extracted beams with millisecond spill duration by means of Beam Current Transformers (BCTs) [2]. In slow extracted beams Secondary Emission Monitors (SEMs) [3] have to be used to get the absolute flux of protons hitting the target. SEMs work on the principle that electrons are liberated from the surface of some solid material when crossed by charged particle beams. They are made of metallic foils (aluminium and titanium, so far) and they are less accurate, less stable, and more difficult to calibrate than BCTs.

The only absolute calibration of the responses of the SEMs used for the T2, T4, and T6 targets of the SPS North Area was performed in 1979, prompted also on that occasion by the needs of an experiment (NA20 [4]), with aims very similar to those of SPY, but located on the H2 beam line derived from the T2 target station. Since that time it has been found that SEMs made of aluminium foils exhibit an ageing effect, i.e. a decrease over time of their electron emission efficiency in the region continuously bombarded by the incident proton beam. Because of these findings, in the middle of 1995 SEMs made of titanium foils were added in front of the T2, T4, and T6 targets. The behaviour in time of these new titanium foils is being carefully followed and up to now they do not seem to suffer from ageing effects [5]. The values of proton intensities for the North Area targets currently displayed on the SPS status monitors ('SPS Page 1') and acquired by the experiments come now from the titanium SEMs. It has so far been assumed that the same calibration constants apply to both types of SEMs.

In order to reduce to the few per cent level the uncertainty on the primary proton intensity hitting the target used for the SPY experiment, a new calibration of the aluminium and titanium SEMs in front of T4 was needed. It was decided to take this opportunity to perform a calibration of all the monitors of the three targets in the North Area. Following the same procedure used in 1979 [6], the SEMs were calibrated by an activation method. The absolute intensity of the proton beam, needed for this calibration, is measured from the radioactivity induced in aluminium foils through which the beam has passed. The foil activity is calibrated in fast extracted beams the intensity of which is measured by BCTs. For this purpose, aluminium foils were first exposed for about 100 SPS spills (corresponding to an integrated intensity of about 10^{14} protons) to the TT60 fast extracted proton beam [Fig. 1(b)] in the West Area Neutrino Facility (WANF), which is equipped with two BCTs. Then, for each of the T2, T4, and T6 targets in the North Area, identical aluminium foils were exposed to comparable integrated proton intensities and the corresponding SEM signals were recorded. From the measured activity of the foils, the collected proton intensity on each target was determined and the calibration factor of each SEM could be obtained.

In Section 2 we shall give a description of the SEMs and their arrangement for the North Area targets. We shall then describe in some detail the activation method and the procedure followed for the measurement of the induced radioactivity (Section 3.1), the reference activation measurements after the exposure of the foils to the WANF fast extracted proton beam (Section 3.2), and the activation measurements after the irradiation of the foils in front of the T2, T4, and T6 targets (Section 3.3). A careful monitoring of the SEMs during the NA56 data taking period was performed in order to check the stability of the measured calibration factors and this is described in Section 3.4. Section 3.5 summarizes our measurements of the calibration factors and secondary emission efficiencies. Our conclusions are presented in Section 4.

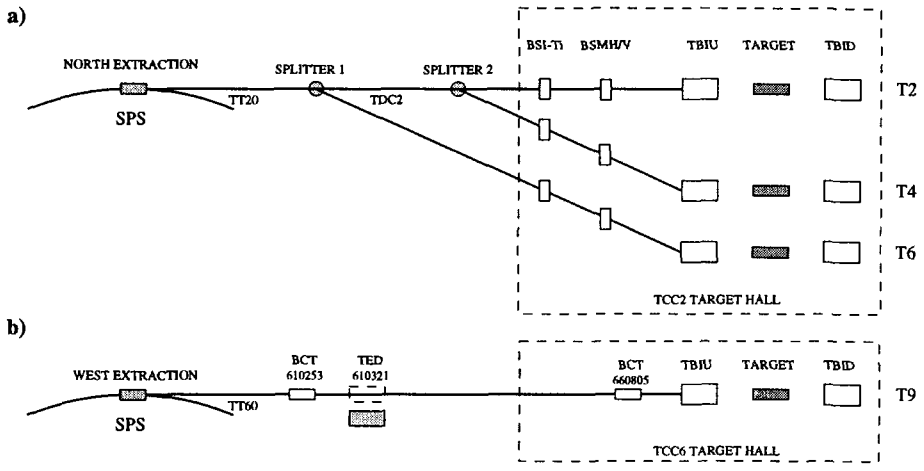

Fig. 1: a) Extraction lines to the North Area targets T2, T4, and T6 and arrangement of the TBIU, TBID, BSMH/V, BSI-Ti boxes containing the SEM foils; b) Extraction line to the West Area neutrino target and arrangement of the TBIU and TBID boxes and of the BCTs. The motorized beam stopper (TED) is also shown.

2 SECONDARY EMISSION MONITORS

2.1 Principle of operation

Secondary emission of electrons from the surface of a plate crossed by a charged particle beam is used as a method to monitor the beam intensity [3]. The liberated charge comes mainly from delta rays escaping from the plate, with a small contribution due to the secondaries produced in the interactions of the beam particles with the plate. The total collected charge has been measured to be proportional to the intensity of the impinging beam. A bias voltage of 200 V/cm is usually applied to the secondary emission plates to make sure that the liberated electrons are quickly collected, so as to avoid the formation of an electron cloud close to the surface of the emitting material. The performance of a SEM is characterized by the secondary emission efficiency $\epsilon_{\rm SEM}$, that is the ratio of the number of electrons $N_{\rm e}$ liberated from the detector foil to the number of charged beam particles (usually protons) $N_{\rm p}$ crossing the foil:

$$\epsilon_{\rm SEM} = N_{\rm e}/N_{\rm p} \ . \tag{1}$$

The SEMs employed in the monitoring of the North Area beams are made of metallic foils (aluminium or titanium), of which both sides are used to collect the liberated electrons. Figure 2 shows a scheme of a SEM and its readout chain. Mechanical and electronic characteristics of the North Area SEMs are summarized in Table 1. The amplitude V of the signal present at the input of the ADC is related to the number $N_{\rm e}$ of electrons liberated from the SEM foil by:

$$V = \frac{qN_{\rm e}G}{C} = \frac{q\epsilon_{\rm SEM}N_{\rm p}G}{C} \simeq 0.8 \ {\rm V}/10^{12} \ {\rm protons} \tag{2}$$

where q is the electron charge, C is the integrator capacitance, and G is the amplifier gain. The numerical value has been computed for $\epsilon_{\rm SEM} \simeq 4\%$, which is a typical value for the North Area aluminium SEMs. Given the ADC sensitivity reported in Table 1, such SEMs can operate in the range from about 10^{10} to 10^{13} protons/pulse.

The result of our measurement is a SEM calibration factor $C_{\rm SEM}$, defined as the ratio of the number $N_{\rm p}$ of protons crossing the detector foil to the corresponding SEM signal $N_{\rm SEM}$ expressed in ADC counts:

$$C_{\rm SEM} = N_{\rm p}/N_{\rm SEM} \ . \tag{3}$$

This C_{SEM} factor is given in terms of the secondary emission efficiency and of the characteristics of the electronic chain by:

$$C_{\mathrm{SEM}} = \frac{CS_{\mathrm{ADC}}}{q\epsilon_{\mathrm{SEM}}G} \tag{4}$$

where the $S_{\mathrm{ADC}} = V/N_{\mathrm{SEM}} \simeq 4.88 \times 10^{-3}$ V/ADC count is the ADC sensitivity from Table 1. A typical C_{SEM} value for the North Area aluminium SEM is about 6.5×10^9 protons/SEM count.

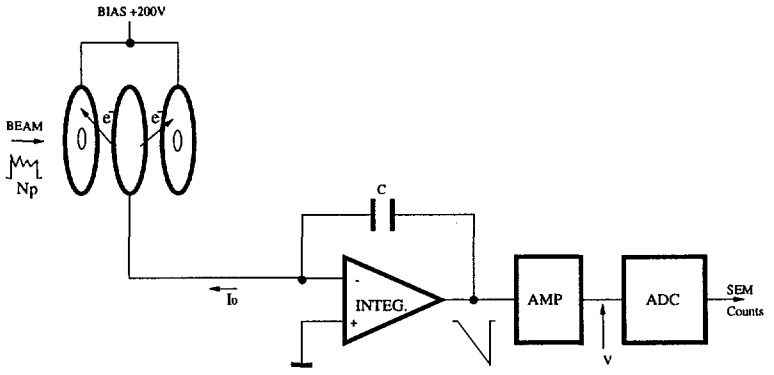

Fig. 2: Scheme of a North Area SEM and its readout chain.

Table 1: Mechanical and electronic characteristics of the North Area SEMs

Foil diameter	145 mm
Foil thickness	20 μm
Electron collection gap	10 mm
Bias voltage	200 V
Integrator capacitance	33 nF
Amplifier gain	3.92
ADC full scale	10 V $\equiv$ 2047 counts
Gain uniformity of channels	$\pm$0.5%
Noise level (detector + cables)	$\pm$1.5 count
Operating range	$10^{10} \div 10^{13}$ protons/pulse

2.2 SEMs for the T2, T4, and T6 targets in the North Area

The T2, T4, and T6 targets in the North Area are each equipped with instrumentation boxes which contain secondary emission monitors and are located immediately upstream (TBIU) and downstream (TBID) of the targets [Fig. 1(a)]. Each of these boxes contains SEMs of different shapes, as shown in Fig. 3. There are monitors made of foils of round shape (BSI) to record the intensity of the proton beam, monitors made of split foils (BSPV and BSPH) to measure the vertical and horizontal beam position, and monitors made of foils with central holes (BSH and BSHS) to give an estimate of the beam halo. All of the monitors in the TBIU and TBID boxes are made of aluminium foils.

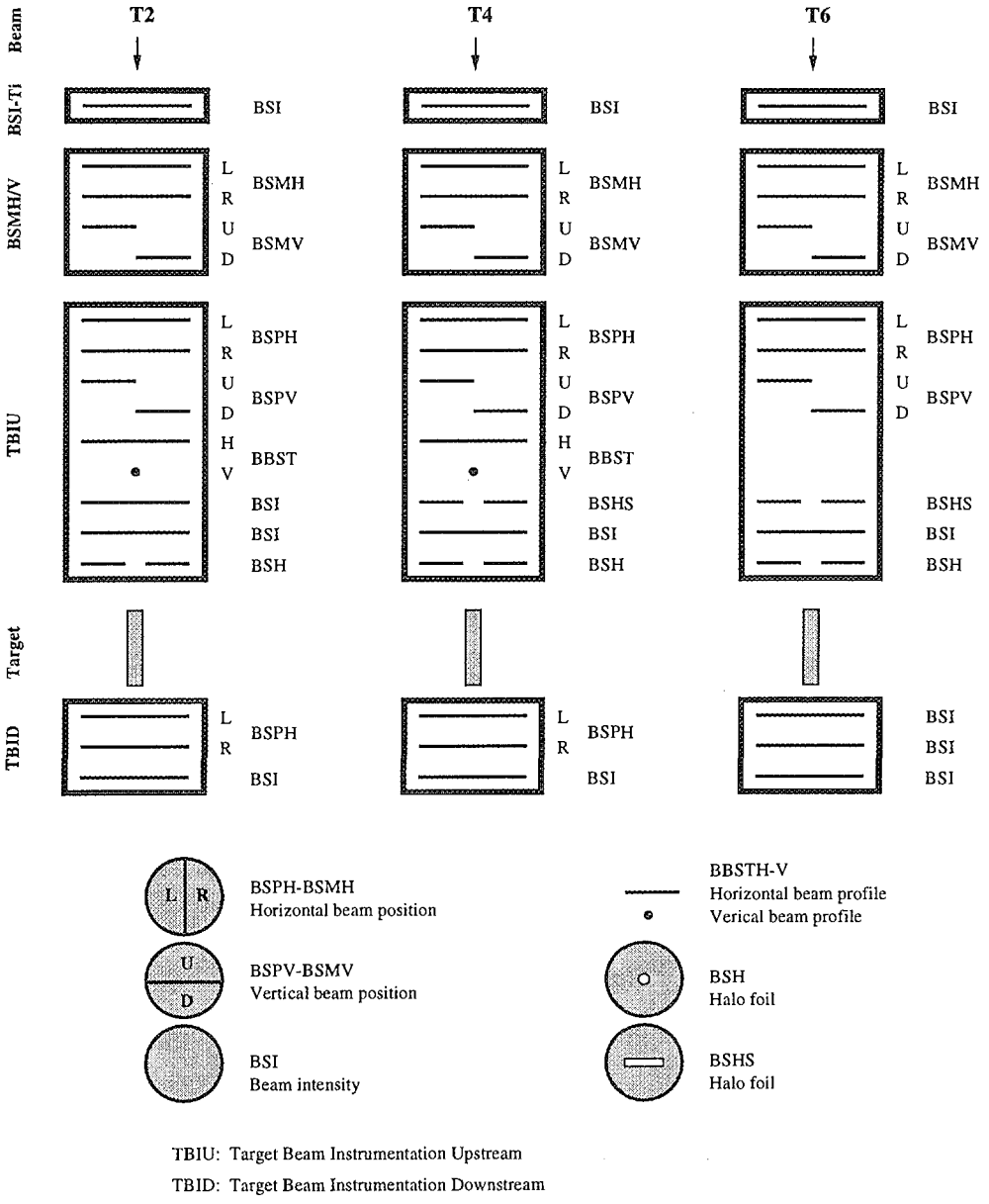

Fig. 3: Detailed SEM foil arrangement in the TBID, TBIU, BSMH/V, BSI-Ti boxes for the T2, T4, and T6 targets.

Additional monitors are present further upstream of each target [Figs. 1(a) and 3]. A set of aluminium split foils (BSMH/V) monitors the angle of incidence of the proton beam on the target. In the middle of 1995 in each beam line, upstream of the BSMH/V foils, a round foil made of titanium (BSI-Ti) was added to provide an additional measurement of the primary proton beam intensity.

Table 2 gives a summary of the positions of the monitors of the T2, T4, and T6 targets, where negative and positive coordinates are used for upstream and downstream positions from the centre of the target, respectively.

We were especially interested in the calibration of the round BSI aluminium foils in the TBIU boxes and of the upstream BSI-Ti titanium foil, because these are the ones used to measure the intensity of protons hitting the target.

Table 2: North Area SEM positions

	Distance from T2 (m)	Distance from T4 (m)	Distance from T6 (m)
TBID	+0.475	+0.475	+0.475
TBIU	−0.525	−0.525	−0.525
BSMH/V	−25.9	−25.9	−15.5
BSI-Ti	−42.3	−53.9	−38.7

3 SEM CALIBRATION

3.1 Activation method

The intensity of particles in a proton beam can be measured by assaying the amount of ^{24}Na produced in an aluminium foil through which the beam has passed. The cross-section σ of the reaction ^{27}Al(p,3pn)^{24}Na for the production of ^{24}Na from aluminium by high-energy protons at energies close to 400 GeV has been measured to be $\sigma = 8.1 \pm 0.6$ mb [7]. The half-life of ^{24}Na is 900.0 minutes [8] and it decays to ^{24}Mg by β^- and γ emission (each decay giving rise to two photons of 1.369 and 2.754 MeV). The ^{24}Na activity in an aluminium foil is conveniently measured by placing the foil close to a 3″ diameter by 3″ high sodium iodide crystal and measuring the number of counts N_c in the 2.754 MeV full-energy peak in the pulse-height spectrum. The number of counts N_c, measured during a time t_c in a foil irradiated for a time t_i, after a time t_e from the end of irradiation, is related to the number φ of incident protons per second by [9, 10]:

$$N_c = \epsilon A_{sat} \tau (1 - e^{-t_i/\tau})(1 - e^{-t_c/\tau}) e^{-t_e/\tau} \tag{5}$$

where:

τ is the lifetime of ^{24}Na

ϵ is the counting efficiency of the sodium iodide crystal

$A_{sat} = \varphi \sigma \rho_{Al} \delta N_{Av} / A_{Al}$ is called saturation activity and corresponds to the activity measured at $t_e = 0$ in the case of a very long irradiation time ($t_i \rightarrow \infty$)

ρ_{Al} is the aluminium density

N_{Av} is the Avogadro constant

A_{Al} is the aluminium atomic weight

δ is the foil thickness.

An absolute determination of φ thus requires an accurate knowledge of the counting efficiency ϵ of the sodium iodide crystal at the energy of 2.754 MeV. This is not often known to an accuracy of better than a few per cent, and taken with the error in the cross-section, larger than 5%, and the error in measuring the thickness of the aluminium foil, of the order of one or two per cent, it is rarely possible to obtain accuracies in measured proton intensities of better than 10%.

Thus, the method employed here was to expose foils, all taken from the same aluminium roll, to proton beams in which the intensity was known and to the proton beams of unknown intensity. In both cases the induced ^{24}Na activity was measured by placing the foils at the same distance from the same sodium iodide crystal. By placing a foil in a proton beam of known intensity we determine the quantity

$$C_f = \epsilon A_{sat} / \varphi. \tag{6}$$

From the exposure to a proton beam of unknown intensity we measure the quantity $\epsilon A'_{\rm sat}$ and thus we can determine, assuming uniform irradiation, the integrated flux of protons $N'_{\rm p} = \varphi' t_{\rm i}$ from

$$N'_{\rm p} = \epsilon A'_{\rm sat} t_{\rm i} / C_{\rm f} \tag{7}$$

where the quantities with a prime are all measured in the exposure to a proton beam of unknown intensity.

Thus any errors in the estimation of proton intensity in the unknown beams are due to statistical inaccuracies in the measurement of the ^{24}Na activity, to the unevenness of the aluminium foil thickness, and to the accuracy of the reference proton beam intensity. Final accuracies of better than a few per cent should be achievable.

Aluminium foils of 10×10 cm^2 and 45 μm thickness were exposed in a sandwich of three foils. Only the centre foil of the sandwich was measured. This technique compensates for the loss by elastic scattering of ^{24}Na recoil nuclei from the measured foil.

The point of impact of the proton beam on the foil was determined by contact radiography using ordinary polaroid film, the beam spot being visualized from the effect on the film of the intense short-lived beta activity soon after the irradiation. A circular disc of aluminium, 3.5 cm in diameter, was cut from the foil so that the beam spot was at the centre of the disc. The rest of the foil was then compressed and also assayed for ^{24}Na activity, since this isotope can also be produced by low-energy (> 6 MeV) neutrons. These neutrons are generated by back-scatter from nearby objects struck by the proton beam (targets, dumps, etc.), thus producing a background activity which has to be subtracted from the measured activity in the beam foil. In the present series of measurements this background activity was never more than 1% of the beam foil activity.

3.2 Reference measurements in the WANF

Aluminium foils were exposed to the WANF fast extracted proton beam in order to normalize the radioactivity induced in the foils to the proton intensity measured by the BCTs. The WANF proton beam serving the T9 neutrino production target is equipped with two BCTs [see Fig. 1(b)] which are capable of measuring absolute proton intensities with a systematic uncertainty of 1.5%. The first one, BCT610253 (hereafter designated by BCT1), has been located since 1976 at the beginning of the TT60 transfer tunnel, just upstream of the location where a motorized beam stopper (TED) can be moved in the beam. The second one, BCT660805 (hereafter called BCT2), identical to the first, was installed early in 1995 just upstream of T9. Specifications for the BCTs are summarized in Table 3.

Table 3: Principal specifications of BCT610253 and BCT660805 (ppp = protons per pulse)

LF cut-off	1 Hz
HF cut-off	20 KHz
Systematic precision	$\pm 1.5\%$
Resolution	1.0×10^{10} ppp

In order to benefit from both devices, two different measurements where carried out with foils close to BCT1 and BCT2, respectively. On 2 April 1996, foils were irradiated in front of the TED beam stopper, moved into the beam, and the integrated proton intensity was measured by BCT1. On 10 April, a second exposure took place just in front of the T9 target, and the information on the accumulated proton intensity could be recorded from both BCT1 and BCT2. Details of the measurements in front of the TED and the T9 target are summarized in Tables 4 and 5 respectively, where we make use of the notations introduced in Section 3.1.

Table 4: Calibration in front of the TED beam stopper in the WANF. BCT measurements are affected by a systematic error of 1.5% (cps = counts/s, pps = protons/s)

Number of SPS pulses		100
Irradiation time (min)		23.76
Total number of protons from BCT1		4.0301×10^{14}
	Mass (g)	$\epsilon A_{\rm sat}$ (cps)
Beam foil	0.1072	1822.1 ± 5.5
Surround foil	1.0853	191.50 ± 0.84
Net $\epsilon A_{\rm sat}$ (cps)		1803.2 ± 5.5
$C_{\rm f}$ (cps/pps)		$(6.379 \pm 0.019 \pm 0.096) \times 10^{-9}$

Table 5: Calibration in front of the WANF T9 target. BCT measurements are affected by a systematic error of 1.5% (cps = counts/s, pps = protons/s)

Number of SPS pulses		103
Irradiation time (min)		24.48
Total number of protons from BCT1		4.5747×10^{14}
Total number of protons from BCT2		4.4607×10^{14}
	Mass (g)	$\epsilon A_{\rm sat}$ (cps)
Beam foil	0.1071	1930 ± 15
Surround foil	1.1015	24.76 ± 0.45
Net $\epsilon A_{\rm sat}$ (cps)		1928 ± 15
$C_{\rm f}$ from BCT1 (cps/pps)		$(6.189 \pm 0.049 \pm 0.093) \times 10^{-9}$
$C_{\rm f}$ from BCT2 (cps/pps)		$(6.347 \pm 0.050 \pm 0.095) \times 10^{-9}$

In both exposures the value of $C_{\rm f}$ [Eq. (6)] was measured, with an error made up of two different contributions. The first one is the uncertainty in the determination of the activity of the irradiated foil and the second one is the 1.5% systematic error on the BCT measurement. In the exposure in front of the T9 target, the 2.5% higher reading of BCT1 compared to BCT2 is most probably explained by beam losses occurring between the positions of the two devices. Losses higher than usual are not surprising since at the time of the measurement (shortly after the yearly start-up of the SPS accelerator) the beam extractions had not yet been satisfactorily tuned. Moreover, quite a good agreement is observed between the value of $C_{\rm f}$ measured in the TED exposure, where the proton intensity is given by BCT1, and the value determined in the T9 exposure, if we take the proton intensity measurement by BCT2. The final $C_{\rm f}$ value has been computed as weighted mean of these two measurements, obtaining:

$$C_{\rm f} = (6.364 \pm 0.072) \times 10^{-9} \text{cps/pps} \tag{8}$$

where cps = counts/s and pps = protons/s.

3.3 SEM calibration in the T2, T4, and T6 beam lines

In order to calibrate the secondary emission monitors, aluminium foils of the same thickness as those used in the WANF beam line were irradiated in front of the T2, T4, and T6 targets of the SPS North Area. During the exposure the signals $N_{\rm SEM}$, expressed in ADC counts, of all the SEM foils installed in the three

beam lines were recorded and the activities induced in the aluminium foils were subsequently measured. The SEM calibration factors C_{SEM} could be computed according to Eqs. (7) and (3).

The procedure of SEM calibration was repeated twice to check the systematic errors of the measurement procedure and to investigate for possible drifts of the SEM calibration factors, particularly for the recently installed SEM titanium foils. A first calibration was carried out on 14 April, about 10 days before the beginning of the SPY data taking, and the second one was performed on 2 May, close to the end of the SPY data taking period. For each of the T2, T4, and T6 targets, the dependence on time (SPS pulse number) during the irradiation of the BSI-Ti signal, expressed in ADC counts, and of the ratio of the BSI to the BSI-Ti signal are shown in Figs. 4 and 5 for the 14 April and 2 May calibration, respectively. Except for a few missing spills, the proton beam intensity was quite stable during the irradiations.

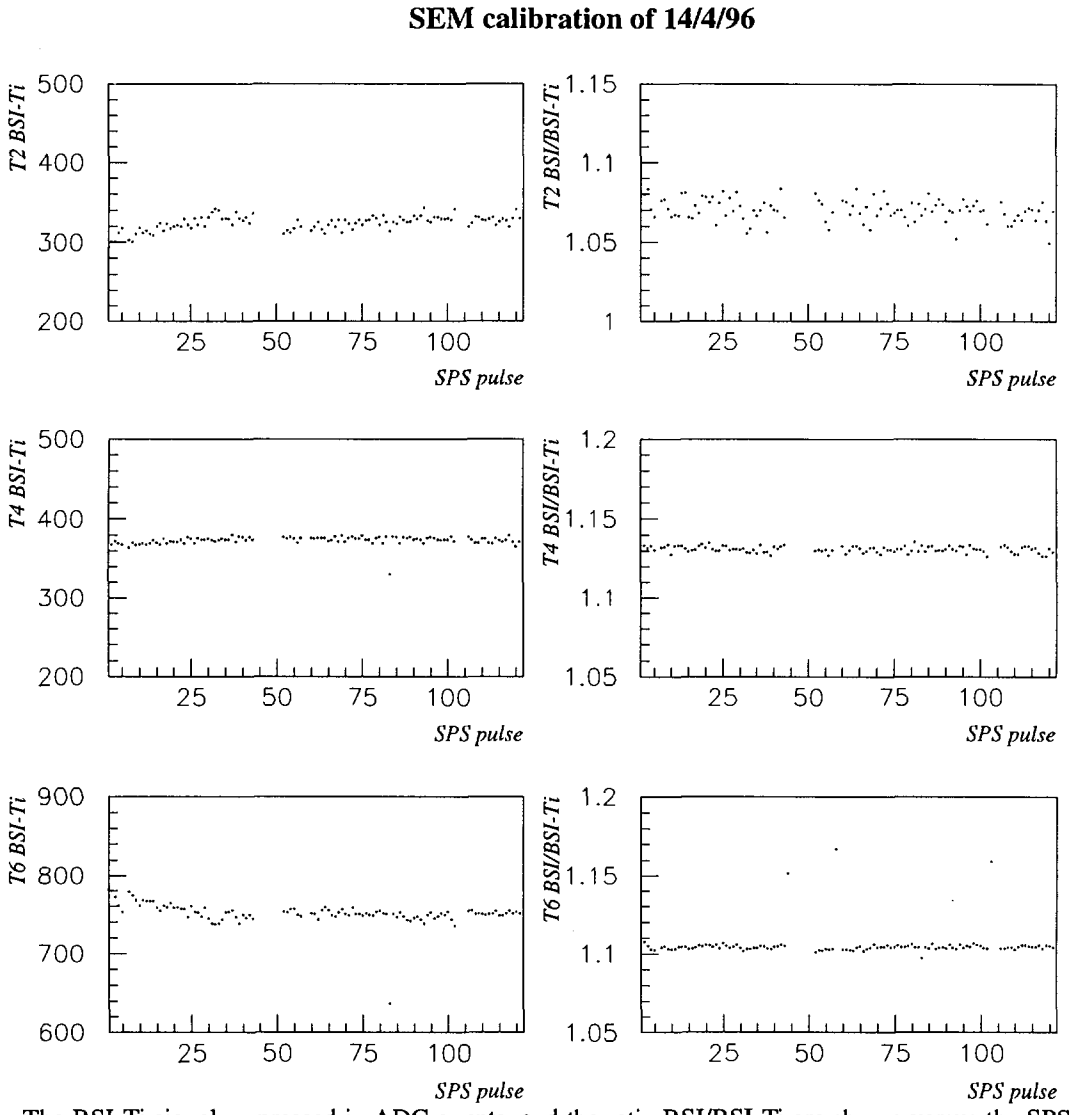

Fig. 4: The BSI-Ti signal, expressed in ADC counts, and the ratio BSI/BSI-Ti are shown versus the SPS pulse number during the irradiation of 14 April 1996, for the T2, T4, and T6 targets.

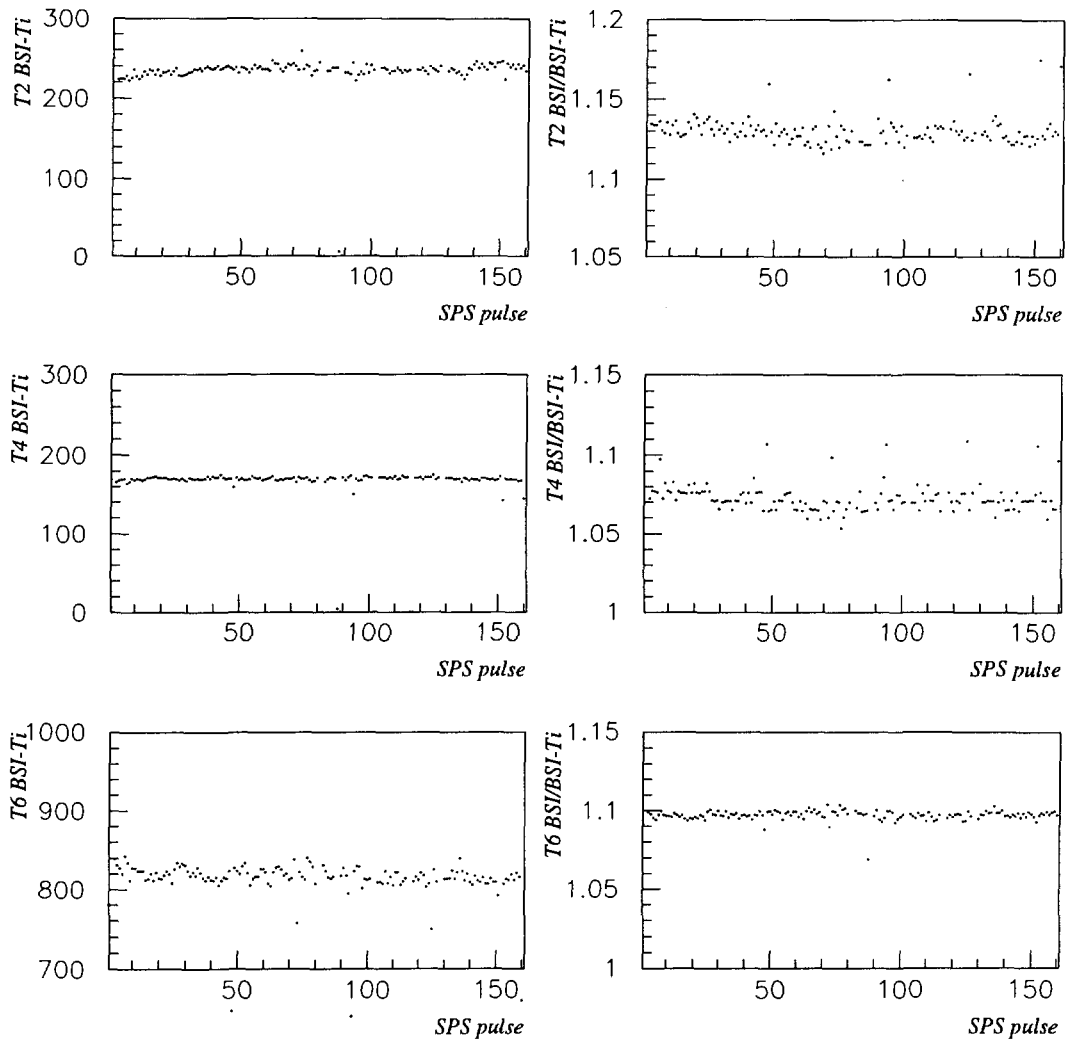

Fig. 5: As for Fig. 4 for the irradiation of 2 May 1996.

A summary of the calibration measurements is reported in Tables 6, 7, and 8 for the round aluminium BSI and for the round titanium BSI-Ti foils of the T2, T4, and T6 targets, respectively. The quoted errors on the total number of protons and on the $C_{\rm SEM}$ calibration factors are split into three different contributions: the uncertainty on the measurement of the activity of the irradiated foil, the thickness unevenness of the different foils cut from the same aluminium roll (measured to be 0.8%), and the error on the $C_{\rm f}$ factor measured in the WANF exposure.

Table 6: SEM calibration in the T2 beam line (cps = counts/s, pot = protons on target)

	Calibration of 14 April 1996		Calibration of 2 May 1996	
Number of SPS pulses	121		160	
Irradiation time (min)	28.80		38.16	
	Mass (g)	$\epsilon A_{\mathrm{sat}}$ (cps)	Mass (g)	$\epsilon A_{\mathrm{sat}}$ (cps)
Beam foil	0.1059	780.1 ± 4.2	0.1075	625.9 ± 2.7
Surround foil	1.1010	17.35 ± 0.45	1.0438	12.90 ± 0.31
Net $\epsilon A_{\mathrm{sat}}$ (cps)	778.4 ± 4.2		624.6 ± 2.7	
Total number of protons	$(2.114 \pm 0.011 \pm 0.017 \pm 0.024) \times 10^{14}$		$(2.247 \pm 0.010 \pm 0.018 \pm 0.025) \times 10^{14}$	
	SEM counts	C_{SEM} (pot/SEM count)	SEM counts	C_{SEM} (pot/SEM count)
BSI-Ti	34671	$(6.096 \pm 0.033 \pm 0.049 \pm 0.069) \times 10^9$	35102	$(6.402 \pm 0.028 \pm 0.051 \pm 0.072) \times 10^9$
BSI	37102	$(5.697 \pm 0.031 \pm 0.046 \pm 0.064) \times 10^9$	39673	$(5.664 \pm 0.024 \pm 0.045 \pm 0.064) \times 10^9$
BSI/BSI-Ti counts	1.07		1.13	

Table 7: SEM calibration in the T4 beam line (cps = counts/s, pot = protons on target)

	Calibration of 14 April 1996		Calibration of 2 May 1996	
Number of SPS pulses	121		160	
Irradiation time (min)	28.80		38.16	
	Mass (g)	$\epsilon A_{\mathrm{sat}}$ (cps)	Mass (g)	$\epsilon A_{\mathrm{sat}}$ (cps)
Beam foil	0.1090	1049.0 ± 6.0	0.1067	491.7 ± 2.5
Surround foil	1.0968	17.67 ± 0.36	1.0507	6.25 ± 0.22
Net $\epsilon A_{\mathrm{sat}}$ (cps)	1047.2 ± 6.0		491.1 ± 2.5	
Total number of protons	$(2.843 \pm 0.016 \pm 0.023 \pm 0.032) \times 10^{14}$		$(1.767 \pm 0.009 \pm 0.014 \pm 0.020) \times 10^{14}$	
	SEM counts	C_{SEM} (pot/SEM count)	SEM counts	C_{SEM} (pot/SEM count)
BSI-Ti	39945	$(7.118 \pm 0.041 \pm 0.057 \pm 0.081) \times 10^9$	25249	$(6.998 \pm 0.036 \pm 0.056 \pm 0.079) \times 10^9$
BSI	45180	$(6.294 \pm 0.036 \pm 0.050 \pm 0.071) \times 10^9$	27085	$(6.523 \pm 0.033 \pm 0.052 \pm 0.074) \times 10^9$
BSI/BSI-Ti counts	1.13		1.07	

Table 8: SEM calibration in the T6 beam line (cps = counts/s, pot = protons on target)

	Calibration of 14 April 1996		Calibration of 2 May 1996	
Number of SPS pulses	121		160	
Irradiation time (min)	28.80		38.16	
	Mass (g)	$\epsilon A_{\mathrm{sat}}$ (cps)	Mass (g)	$\epsilon A_{\mathrm{sat}}$ (cps)
Beam foil	0.1053	2162 ± 17	0.1062	2425.0 ± 9.0
Surround foil	1.0763	80.6 ± 1.5	1.0500	84.72 ± 0.50
Net $\epsilon A_{\mathrm{sat}}$ (cps)	2154 ± 17		2416.4 ± 9.0	
Total number of protons	$(5.849 \pm 0.046 \pm 0.047 \pm 0.066) \times 10^{14}$		$(8.694 \pm 0.032 \pm 0.070 \pm 0.098) \times 10^{14}$	
	SEM counts	C_{SEM} (pot/SEM count)	SEM counts	C_{SEM} (pot/SEM count)
BSI-Ti	80534	$(7.262 \pm 0.057 \pm 0.058 \pm 0.082) \times 10^9$	121017	$(7.184 \pm 0.027 \pm 0.057 \pm 0.081) \times 10^9$
BSI	88917	$(6.578 \pm 0.052 \pm 0.053 \pm 0.074) \times 10^9$	132784	$(6.547 \pm 0.024 \pm 0.052 \pm 0.074) \times 10^9$
BSI/BSI-Ti counts	1.10		1.10	

3.4 Long-term stability

In order to investigate possible drifts of the SEM responses, two independent calibrations were performed for the SEM foils of all the North Area targets at an interval of about 20 days, as reported in the preceding section. Additional valuable information comes from the monitoring of the signal ratio of two different SEM foils crossed by the same proton beam. This study was especially performed for the SEMs equipping the T4 target. Their signals were recorded for each SPS pulse in the period from 17 April to 12 May, which includes the SPY data taking period of 25 April to 6 May.

The ratio of the T4 BSI to the BSI-Ti signal shows (Fig. 6) sudden jumps at the few per cent level during a period of a few hours. Analogous jumps are present in the signal ratios of all the TBIU SEMs to the BSI-Ti foil. A careful investigation has shown these jumps to be correlated with the change of target type during SPY data taking. Three different Be plates were used, 160 mm wide, 2 mm high and of different length along the beam line direction (100, 200 and 300 mm). In addition a target was used consisting of three spare T9 Be rods of 100 mm length and 3 mm in diameter interleaved by 90 mm of air [1]. The behaviour is such that the ratios of the TBIU SEMs to the BSI-Ti signal show values increasing with the length of the Be target in use and when no target is present they have the smallest values. This suggests a contribution to the signals of all the TBIU SEM foils due to backward-going particles, produced by proton interactions in the target. In addition, as reported in Table 2, the TBIU sits at about half a metre from the centre of each target, so that the upstream edge of a longer target is nearer to the TBIU, with a larger solid-angle acceptance for backward-going particles.

In order to check the stability of the ratio of the T4 BSI to the BSI-Ti signal we had to select data corresponding to a given target type. Figure 7 shows this ratio, for some periods of time chosen throughout SPY data taking when the 300 mm Be target was in use, as a function of the horizontal asymmetry measured by the BSPH foils. A given value of the split foil asymmetry corresponds to a precise beam position for a beam of stable dimension. The vertical asymmetry BSPV(U−D)/(U+D) was required to be 0.50 ± 0.05, so as to have the beam hitting the BSI foil at a constant vertical position. The plot shows clearly that the BSI foil, as was previously known [5], suffers from a position-dependent efficiency due to a beam-related ageing effect. The spread of the ratio of the BSI to the BSI-Ti signal for the different data periods, at a same value of the horizontal asymmetry, is within $\pm 1\%$, and a close inspection shows no systematic time drift of such a ratio.

The study of the long-term stability of the SEM calibration factors is better achieved if we monitor the ratio of the sum of the signals of the BSM split foils to the BSI-Ti signal, so as not to be dependent on the target backscattering which affects all the TBIU foils. In addition we have to select data corresponding to a well-defined beam position on the BSM foils, because all the aluminium foils show a position-dependent efficiency because of the ageing effect. We have chosen the following asymmetry intervals, which cover a fair part of the available data: BSMV(U−D)/(U+D) = 0 ± 0.15 and BSMH(L−R)/(L+R) = -0.15 ± 0.05. Within these limits, the mean values of the ratios BSMV(U+D)/BSI-Ti and BSMH(L+R)/BSI-Ti are shown in Fig. 8 for each available day from 17 April to 12 May. They are stable within $\pm 1\%$ and an analysis of the time dependence of these values shows that any systematic time drift of the calibration factor of the T4 BSI-Ti foil is at most 0.5% over a period of 26 days.

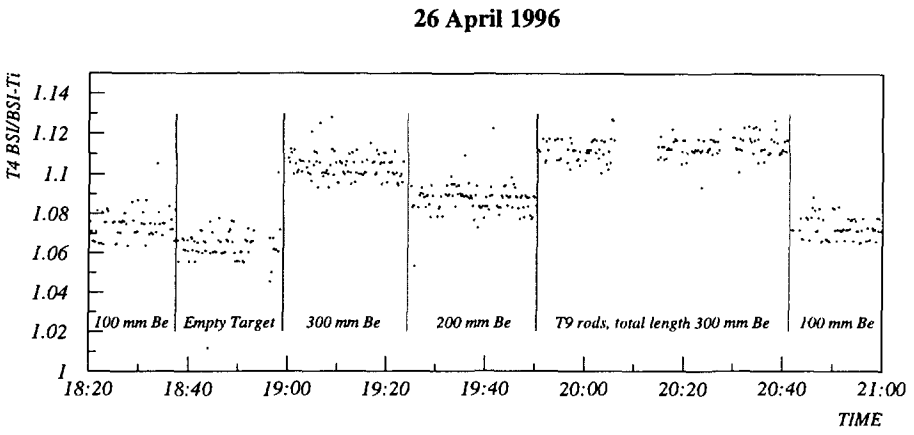

Fig. 6: Ratio of the BSI to the BSI-Ti signal for the T4 target as a function of time during a period of a few hours on 26 April 1996.

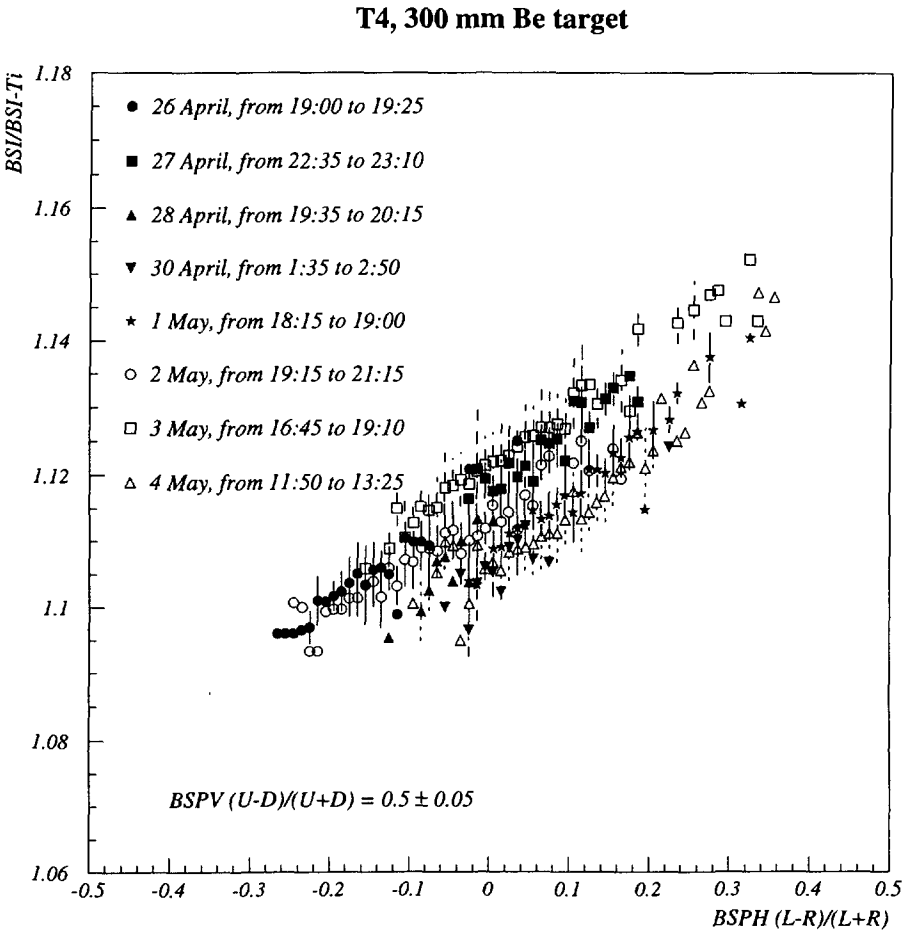

Fig. 7: Ratio of the BSI to the BSI-Ti signal for the T4 target as a function of the horizontal asymmetry measured by the BSPH foils. The error bar on each point gives the observed spread of the ratio BSI/BSI-Ti around the mean value.

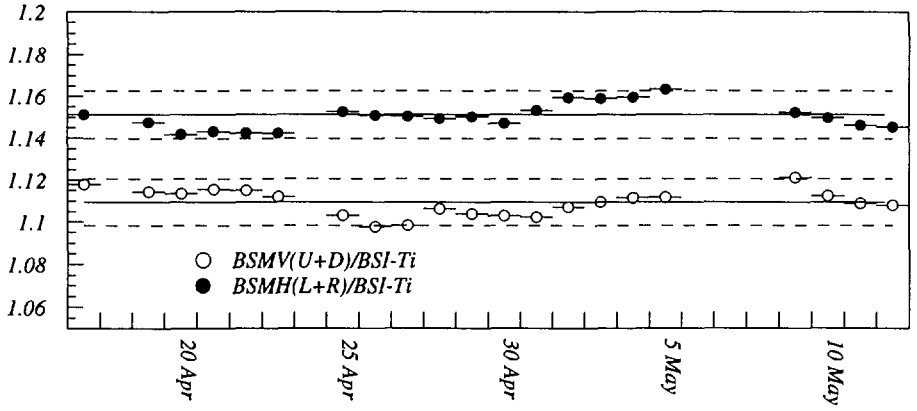

Fig. 8: Ratio of the sum of the BSMV split foils to the BSI-Ti foil (white circles) and of the sum of the BSMH split foils to the BSI-Ti foil (black circles) for the T4 target as a function of day from 17 April to 12 May. The mean value of each ratio (full lines) and the $\pm 1\%$ variation (dotted lines) are also shown.

3.5 Summary of calibration factors and secondary emission efficiencies

Both BSI and BSI-Ti calibration factors are summarized in Table 9, where the first two contributions to the errors reported in Tables 6, 7, and 8 are here combined together in a single number that expresses the error related to each irradiation measurement and the common error coming from the uncertainty on the C_{f} factor is left separate. The C_{SEM} factor reported under the column 'Final value' has been computed as a weighted mean of the two measurements if these are consistent within the errors. The T2 BSI-Ti and the T4 BSI foils show a difference between the two successive measurements of 5% and 3.5%, respectively, which exceeds the estimated error. In such cases we give the mean value of the two distinct measurements and its standard deviation. The disagreement in the case of the T4 BSI foil is in large part due to the fact that different targets were being used during the calibrations on 14 April and 2 May, that is the 300 mm Be and the 100 mm Be target, respectively. As shown in Fig. 6, the difference in the backscattering contribution from these two targets could explain quantitatively the discrepancy in the measured calibration factors. We still have no explanation for the behaviour of the T2 BSI-Ti foil: and even in the worst case, the errors on the SEM calibration factors do not exceed 3%.

The secondary emission efficiencies of the BSI and BSI-Ti foils, computed from the final C_{SEM} factors [see Eq. (4)], are also shown in Table 9. The first contribution to the error takes into account the uncertainty related to the irradiation measurements of each North Area target and the spread in gain of the electronic channels, as given in Table 1. The second contribution to the error is the common uncertainty coming from the error on the C_{f} factor. We expect secondary emission efficiencies to be the same for all foils of a given material (aluminium or titanium). This is true, within the estimated errors, for the BSI-Ti foils of the T4 and T6 targets. There is also agreement between the efficiencies of the BSI foils of the T4 and T6 targets, within the larger estimated error for the T4 target. However, both the BSI and BSI-Ti foils of the T2 target show values which are 14% higher than the corresponding ones measured for the T4 and T6 targets. This would be the case if the primary proton beam feeding the T2 target were contaminated by other particles (e.g. muons, electrons), which nevertheless give a signal in the secondary emission monitors, but cannot produce any ^{24}Na in the irradiated aluminium foils. We have no proof for this conjecture, but it is worth while remarking that in the previous SEM calibration in 1979 [6] a 35% higher efficiency was measured for the T2 aluminium SEM compared to the values then obtained for the T4 and T6 aluminium SEMs.

As reported in Table 9, the value of the secondary emission efficiency of the titanium SEM foils installed in 1995 has been measured to be 9% lower than that of the aluminium SEM foils.

Table 9: Summary of SEM calibration factors and secondary emission efficiencies (pot = protons on target).

		Calibration of 14 April 1996	Calibration of 2 May 1996	Final value	
		C_{SEM} (pot/SEM count)	C_{SEM} (pot/SEM count)	C_{SEM} (pot/SEM count)	ϵ_{SEM} (%)
T2	BSI-Ti	$(6.096 \pm 0.059 \pm 0.069) \times 10^9$	$(6.402 \pm 0.058 \pm 0.072) \times 10^9$	$(6.25 \pm 0.15 \pm 0.07) \times 10^9$	$4.11 \pm 0.10 \pm 0.05$
	BSI	$(5.697 \pm 0.055 \pm 0.064) \times 10^9$	$(5.664 \pm 0.051 \pm 0.064) \times 10^9$	$(5.679 \pm 0.038 \pm 0.064) \times 10^9$	$4.520 \pm 0.037 \pm 0.051$
T4	BSI-Ti	$(7.118 \pm 0.070 \pm 0.081) \times 10^9$	$(6.998 \pm 0.066 \pm 0.079) \times 10^9$	$(7.055 \pm 0.048 \pm 0.080) \times 10^9$	$3.638 \pm 0.031 \pm 0.041$
	BSI	$(6.294 \pm 0.062 \pm 0.071) \times 10^9$	$(6.523 \pm 0.062 \pm 0.074) \times 10^9$	$(6.41 \pm 0.11 \pm 0.07) \times 10^9$	$4.01 \pm 0.07 \pm 0.05$
T6	BSI-Ti	$(7.262 \pm 0.082 \pm 0.082) \times 10^9$	$(7.184 \pm 0.063 \pm 0.081) \times 10^9$	$(7.213 \pm 0.050 \pm 0.082) \times 10^9$	$3.558 \pm 0.030 \pm 0.040$
	BSI	$(6.578 \pm 0.074 \pm 0.074) \times 10^9$	$(6.547 \pm 0.058 \pm 0.074) \times 10^9$	$(6.559 \pm 0.046 \pm 0.074) \times 10^9$	$3.914 \pm 0.033 \pm 0.044$

4 CONCLUSIONS

Two independent calibrations, over a period of about 20 days, were performed for the SEMs equipping the T2, T4, and T6 targets of the SPS North Area. For the first time, the titanium monitors, installed in the middle of 1995, have been absolutely calibrated.

Our measurements of the SEM calibration factors are summarized in Table 9. The errors, even in the worst case, do not exceed 3%. The calibration factor of the T4 titanium SEM has been measured with an uncertainty of 1.3%. This represents a substantial improvement with respect to a constant calibration factor of 6.58×10^9 protons/SEM count, applied during 1996 to all the titanium SEM foils of the T2, T4, and T6 targets to get the values of proton intensities displayed on the SPS status monitors ('SPS Page 1') and delivered to the experiments.

Secondary emission efficiencies were computed from the measured calibration factors. The value of the titanium SEM foils is 9% lower than that of the aluminium SEMs.

Both aluminium and titanium SEM foils of the T2 target have 14% higher efficiencies than those measured for the SEMs of the T4 and T6 targets. This might indicate a contamination of the proton beam feeding the T2 target by muons and/or electrons and in this case the SEM calibration factors measured for the T2 target would change according to the contamination level.

The SEM responses of the T4 beam line have been continuously recorded for about one month. The signal ratio of two distinct foils crossed by the same proton beam has been carefully studied to monitor the stability in time of the measured calibration factors. In addition this study showed that, as was previously known [5], the aluminium SEMs suffer from a position-dependent efficiency due to a beam-related ageing effect. Evidence was also found of a backscattering contribution from the target, at the level of a few per cent, on all the SEM foils sitting at about half a metre upstream of the target. Our conclusion is that the recently installed titanium monitors, which sit at about 40 m upstream of the target, are more reliable monitors of the proton beam intensity.

The T4 titanium SEM response was shown to be stable within $\pm 1\%$ over a period of almost one month. By combining this additional uncertainty to the error on the determination of the calibration factor from the activation measurement, the absolute proton intensity delivered to the SPY experiment could thus be measured from the titanium monitor with an uncertainty of 1.7%.

Acknowledgements

Special thanks go to K. Elsener, H. Jakob, and R. Jung for enlightening discussions.

We would like to thank A. Faugier and all the staff of the SL/OP group for allowing us access to the TCC2 and TCC6 target halls and for the stable performance of the SPS during our calibration measurements.

We would like to thank the SL Radiation Protection Section for ensuring safe access to the target halls and providing us with the instrumentation for the measurement of the foil activities.

Files with recorded values of the SEMs have been made available on our computers thanks to the help of M. Clayton.

The financial support of Instituto Nazionale di Fisica Nucleare (Italy) is gratefully acknowledged.

K. Bernier was supported by a grant from F.R.I.A.

References

[1] Measurement of pion and kaon fluxes below 60 GeV/c produced by 450 GeV/c protons on a beryllium target, CERN-SPSLC/96–01, SPSLC/P294, 8 January 1996.

[2] H. Jakob, private communication.

[3] K. Budal, *IEEE Trans. Nucl. Sci.* **14** (1967) 1132.

[4] H.W. Atherton et al., Precise measurements of particle production by 400 GeV/c protons on beryllium targets, CERN 80–07 (1980).

[5] G. Ferioli and R. Jung, Evaluation of the evolution of secondary emission coefficients, contributed paper to the Third European Workshop on Beam Diagnostics and Instrumentation for Particle Accelerators, Frascati, 1997.

[6] A. Chapman-Hatchett et al., Calibration of the secondary emission monitors TBIU and TBID of the North Area target stations T2, T4, and T6 in TCC2 for slow extracted protons of 400 GeV, SPS/ABT/Int. 79–1, 27 April 1979.

[7] S.B. Kaufman, M.W. Weisfield, E.P. Stenberg, B.D. Wilkinson, and D. Henderson, *Phys. Rev.* **C14** (1976) 1121.

[8] International Commission on Radiological Protection, Radionuclide transformations: Energy and intensity of emissions, ICRP Publication 38 (Pergamon Press, Oxford, 1983).

[9] M. Barbier, Induced radioactivity (North-Holland, Amsterdam, 1969).

[10] E. León-Florián, C. Leroy, and C. Furetta, Particle fluence measurements by activation technique for radiation damage studies, CERN/ECP 95–15, 4 August 1995.

List of CERN Reports published in 1997

CERN 97–01
CERN. Geneva
Taylor, L; Vandoni, C E [eds]
HEPVIS96 Workshop on Visualization in High-Energy Physics; CERN, Geneva, Switzerland, 2–4 September 1996
CERN, 29 Jan 1997. – 162 p

CERN 97–02
CERN. Geneva
Jacob, M; Quercigh, E [eds]
The CERN OMEGA Spectrometer, 25 years of Physics; CERN, Geneva, Switzerland, 19 March 1997
CERN, 12 June 1997. – 60 p

CERN 97–03
CERN. Geneva
Ellis, N; Neubert, M [eds]
Proceedings, 1996 European School of High-Energy Physics, Carry-le-Rouet, France, 1–14 September 1996
CERN, 2 June 1997. – 316 p

CERN 97–04
CERN. Geneva
Lawson, J; Brianti, G
50 Years of Synchrotrons
Twelfth John Adams Memorial Lecture delivered at CERN on 7 November 1996
CERN, 2 July 1997. – 80 p

CERN 97–05
CERN. Geneva
Veltman, M
Reflections on the Higgs System
Lectures given in the Academic Training Programme of CERN 1996–1997
CERN, 25 July 1997. – 72 p

CERN 97–06
CERN. Geneva
Gougas, A K; Lemoigne, Y; Pepe-Altarelli, M; Petroff, P; Wulz C E [eds]
Proceedings, First International Four Seas Conference, Trieste, Italy, 26 June – 1 July 1995
CERN, 31 July 1997. – 326 p

CERN 97–07
CERN. Geneva
Bernier, K; de Rijk, G; Ferioli, G; Hatziangeli, E; Marchionni, A; Palladino, V; Stevenson, G.R; Tabarelli de Fatis, T; Tsesmelis, E
Calibration of Secondary Emission Monitors of Absolute Proton Beam Intensity in the CERN SPS North Area
CERN, 3 July 1997. – 22 p

CERN 97–07
ISSN 0007–8328
ISBN 92–9083–119–7